# THE ELECTRICAL BEHAVIORS OF ANTARCTIC ICE DRILLED AT MIZUHO STATION, EAST ANTARCTICA*

Norikazu MAENO

*The Institute of Low Temperature Science, Hokkaido University, Sapporo 060*

***Abstract:*** The electrical properties of Antarctic firn and ice cores drilled at Mizuho Station (70°41′53″S, 44°19′54″E) to the depth of 145 m were studied in a wide range of frequency (0.1 Hz to 1 MHz) and temperature (0 to −50°C). Remarkable differences were found between the cores taken from depths shallower than 55 m and those from deeper parts. Dielectric properties of the cores above 55 m, corresponding to cores permeable to air flow and with densities less than 840 $kg \cdot m^{-3}$, could be explained as those of heterogeneous mixture-dielectrics of ice and air, though the physical meaning of the activation energies, namely $0.20 \pm 0.02$ eV ($19.3 \pm 1.5$ $kJ \cdot mol^{-1}$) for dielectric relaxation and $0.21 \pm 0.02$ eV ($20.3 \pm 1.5$ $kJ \cdot mol^{-1}$) for high-frequency conduction, were not clarified completely. Cores deeper than 55 m, corresponding to impermeable cores with densities higher than 840 $kg \cdot m^{-3}$, showed extremely large dielectric constants and conductivities with activation energies of $0.19 \pm 0.02$ eV ($18.4 \pm 1.5$ $kJ \cdot mol^{-1}$) and $0.23 \pm 0.02$ eV ($22.2 \pm 1.5$ $kJ \cdot mol^{-1}$) for dielectric relaxation and high-frequency conduction, respectively. The difference of the electrical properties from those of ordinary pure ice suggests that some unknown mechanism is working in the deep polar ice probably because of the abnormal circumstances due to high hydrostatic pressure and high homologous temperature, coupled with the sophisticated stress field.

Based on the results of the present electrical measurements, the alteration of densification mechanisms was suggested to occur at a depth around 30 m corresponding to the density of 730 $kg \cdot m^{-3}$, where the bonding and compaction of composing ice particles were regarded to have reached their optimum mode, which was also confirmed by petrographic analyses of cores such as areas of internal free surfaces and grain boundaries.

## 1. Introduction

In geophysical resistivity surveys RÖTHLISBERGER (1967) found that electrical conductivities obtained in cold polar glacier ice were by orders of magnitude larger than those of temperate glacier ice and laboratory grown pure ice. Dielectric properties of deep cores taken from cold polar glaciers have been investigated by PAREN (1973), MAENO (1974a, 1974b) and FITZGERALD and PAREN (1975) in a wide

* Contribution No. 1931 from the Institute of Low Temperature Science, Hokkaido University.

range of frequency and temperature, and they found remarkable differences in the dielectric properties from those of pure laboratory ice or temperate glacier ice, *e.g.*, the electrical conductivities of polar ice are larger, relaxation times of the dielectric dispersion are shorter, or the activation energies for high-frequency conductivity and relaxation time are smaller.

The proper understanding of the electrical behaviors of polar ice is essential to interpret data obtained by using various remote sensing techniques such as radio-echo sounding and resistivity surveys, and to develop electric instruments to be used in the polar regions. On the other hand, the study of the electrical properties of drilled polar core samples gives much information on the glaciological history of the ice sheet, especially on the characteristics of formation and ageing processes which might be the main cause of the unusual electrical behaviors mentioned above.

This paper gives detailed results of the electrical measurements carried out on the firn and ice cores drilled at Mizuho Station in East Antarctica, with some references to petrofabric and structural textures of the cores.

## 2. Measurements

### *2.1. Preparation of specimens*

Specimens for the electrical measurements were ice cores drilled at Mizuho Station (70°41′53″S, 44°19′54″E) in East Antarctica by the 12th and 13th Japanese Antarctic Research Expedition (JARE) in 1971 and 1972; cores used in the present measurements ranged from 7 to 140 m in depth and from 550 to 900 $kg \cdot m^{-3}$ in bulk density; the specimens of 7 to 75 m are JARE-12 cores and those of 75 to 140 m are JARE-13 cores.

The ice cores were cut into plates of roughly 5 cm × 5 cm × 0.6 cm in size with a band saw, and two wider surfaces were planed carefully to be exactly in parallel. Because of the limited sizes of the provided cores, the wider surfaces of specimens could only be taken in the vertical direction, *i.e.*, in the same direction as the drilling was conducted: accordingly in the measurements the electric field applied was horizontal to the ice cores.

A specimen was fixed to the electrodes in two different ways: in one method the specimen was directly frozen to the electrodes by minimum thawing and re-freezing, and in the other method thin, about 10 $\mu$m, tin foils were adhered on the both sides of a specimen by using a small amount of lubricant oil (Matsumura Sekiyu Hydol-400) to ensure the complete contact, and then the electrodes were allowed to be in contact with the specimen using a coil spring action. Sometimes the former method caused troubles since it often changed crystallographic and structural textures of permeable low-density specimens and also produced artificial mechanical strains in specimens especially of impermeable high-density core, therefore the latter method was used mostly in the present measurements.

*2.2. Apparatus and procedure of the electrical measurements*

The electrical measurements were conducted at d.c. and frequencies from 0.1 Hz to 1 MHz. The three-terminal circular electrodes were used with a guard-ring. The diameter of the central electrode was 37.0±0.1 mm. The electrical instruments used in the d.c. measurements were an electronic picoammeter (Takeda Riken TR-8641) and a d.c. voltage supplier (Toa Dempa SV-1A), and those used in the a.c. measurements were two bridges (Ando Denki TRS-4 and TRS-10C), oscillators (Ando Denki ULO-5 and WBG-9) and null-detectors (Ando Denki EDC-5 and BDA-9).

Measurements of each sample were conducted at several constant temperatures in a range from 0 to −50°C. To get reproducible results it was necessary to maintain a sample at a constant temperature within an accuracy of ±0.3°C for at least an hour. Details of the electrical apparatus and temperature control were reported in a previous paper by the present author (MAENO, 1973a).

## 3. Results

*3.1. Frequency dependence of dielectric constant and conductivity*

Typical frequency dependence curves of dielectric constant and conductivity measured at −25°C are shown in Figs. 1 and 2 for Mizuho cores of different depths. It is seen in Fig. 1 that values of dielectric constant increase as the depth increases or the frequency decreases, and that the frequency dependence can be classified into two distinct groups: one group shows relatively smaller values of static dielectric constant, namely about 100 at the largest, and the other shows much larger values, of about 1000. Cores recovered from depths shallower than about 50 m belong to the former group, and deeper cores belong to the latter. The depth 50 m cor-

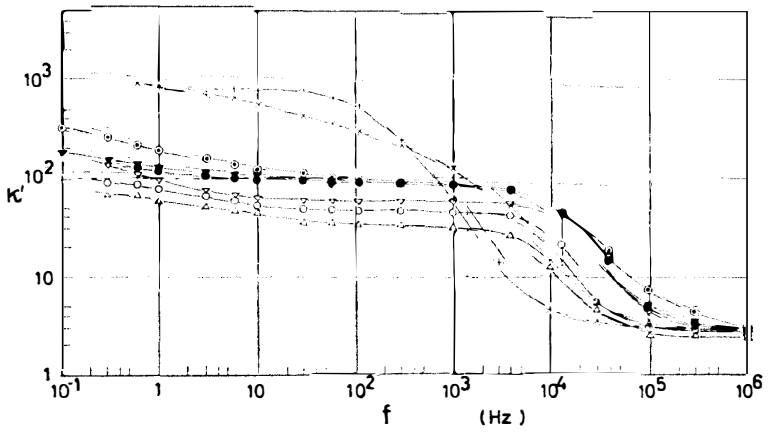


*Fig. 1. Frequency dependence of dielectric constant ($\kappa'$) for the Mizuho cores at different depths. △ (7.8 m, −26.0°C), ○ (10.9 m, −25.2°C), ▽ (18.3 m, −25.3°C), ⊙ (31.1 m, −24.6°C), ● (40.3 m, −25.5°C), ▼ (50.1 m, −25.8°C), + (68.1 m, −25.8°C), × (137.7m, −25.1°C).*

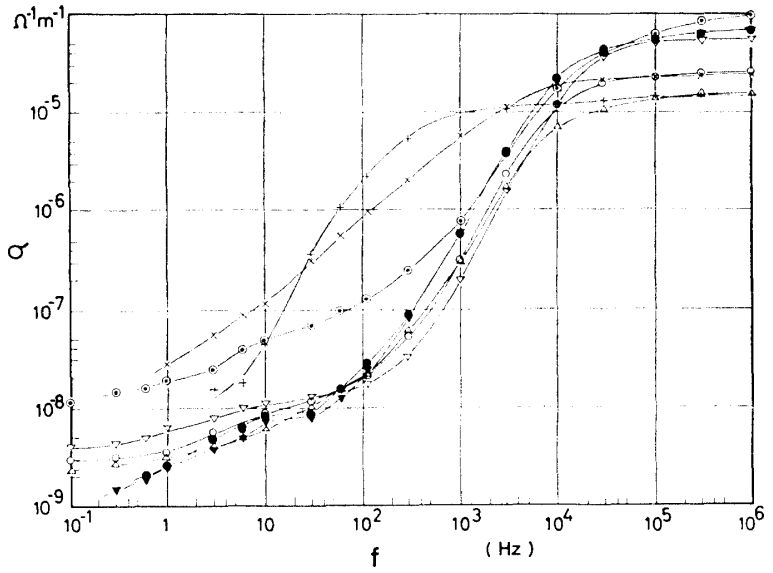


*Fig. 2. Frequency dependence of conductivity ($\sigma$) of the Mizuho cores for different depths. Depths and temperatures of measurements are the same as in Fig. 1.*

responds to the bulk density of 820 kg·m$^{-3}$ (NARITA and MAENO, 1978), but the present measurements suggest that the critical depth dividing the dielectric properties of the Mizuho cores lay around 55 m (840 kg·m$^{-3}$) since all of five specimens from 55 m and 56 m depth showed much larger dielectric dispersions than those from 61 m and 68 m, comparable to those of more deeper Byrd and Amery cores (MAENO, 1974a, 1974b). This specific density coincides with the frequently reported figures at which interconnecting air spaces become completely closed off (PERUTZ and SELIGMAN, 1939; LANGWAY, 1958), which was confirmed actually for the Mizuho cores by petrographic analyses (NARITA *et al.*, 1978).

Characteristics of electrical conductivity is more complicated: Fig. 2 shows that the high-frequency conductivity of the shallow cores is generally larger than that of deep cores, while the low-frequency (d.c.) conductivity of the former is much smaller than that of the latter.

Examinations were made of the dependence of these electrical properties upon the thickness of a specimen, but no dependences were found in the variation of thickness from 4 mm to 9 mm. This implies that effects of polarization due to pile-up of space charges at the electrode-specimen interfaces are not significant, and that the observed dielectric results are primarily attributable to actual phenomena occurring within the specimen.

### *3.2. Temperature dependence of dielectric constant and conductivity*

Figs. 3 and 4 give the temperature dependence of dielectric constant and conductivity for the Mizuho core of 19.6 m and 104.4 m, respectively. In both the

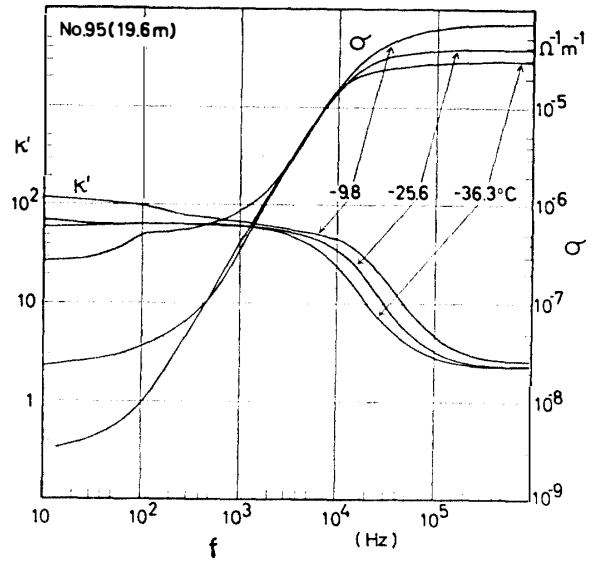


*Fig. 3. Frequency dependence of dielectric constant ($\kappa'$) and conductivity ($\sigma$) of a core of 19.6 m for several different temperatures.*

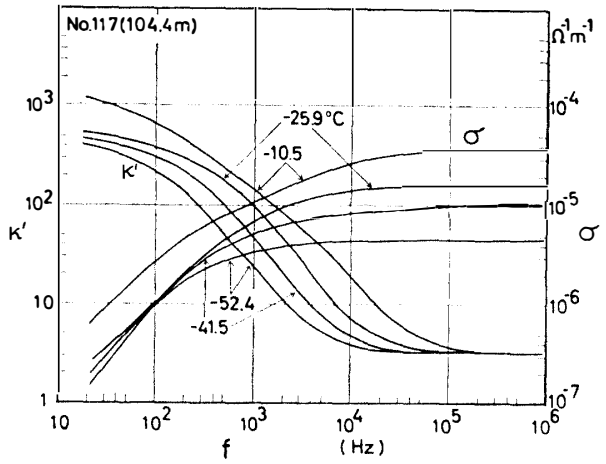


*Fig. 4. Frequency dependence of dielectric constant ($\kappa'$) and conductivity ($\sigma$) of a core of 104.4m for several different temperatures.*

samples, as the temperature was lowered, values of dielectric constant and conductivity were reduced and the whole dielectric dispersion shifted towards the lower frequency range. This tendency implies that the number or mobility of charge carriers, which give rise to each of the dielectric polarizations, decreases as the temperature is lowered.

### *3.3. Cole-Cole plot and static dielectric constant*

To get more insight into variations of the dielectric constant and conductivity with frequency and temperature, dielectric constants ($\kappa'$) and loss factors ($\kappa''$) were

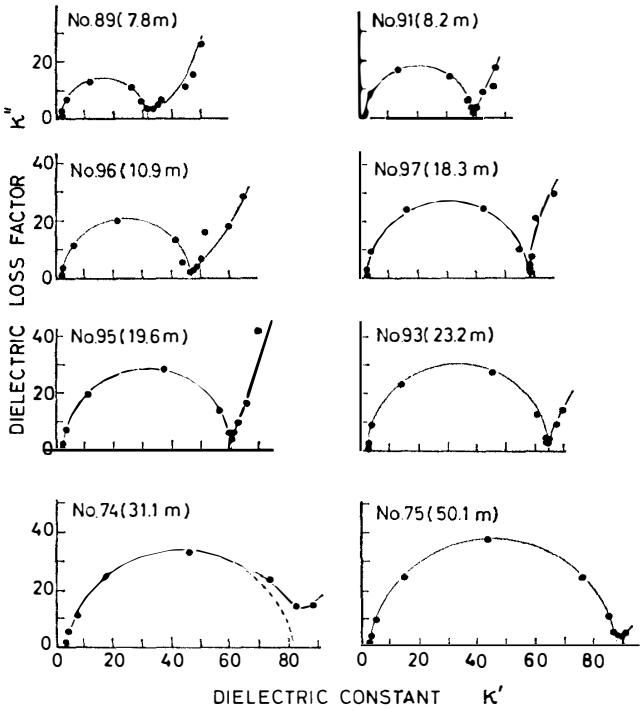


*Fig. 5. Cole-Cole diagrams of complex dielectric constant in complex plane. Temperatures of measurements are −26.0°C (7.8 m), −26.6°C (8.2 m), −25.2°C (10.9 m), −25.3°C (18.3 m), −25.6°C (19.6 m), −25.3°C (23.2 m), −24.6°C (31.1 m), and −25.8°C (50.1m).*

plotted in a complex plane, some examples of which are shown in Fig. 5 for shallower core samples. As seen in the figures the experimental data lie on each semi-circle, which means that these dielectric dispersions can be described in a reasonable manner by the Debye equation with a single relaxation time; in the Debye type dispersion the complex dielectric constant ($\kappa^*$) varies from its static value ($\kappa'_0$) to its high-frequency value ($\kappa'_\infty$) according to the formula

$$\kappa^* = \kappa'_\infty + \frac{\Delta\kappa'}{1+i\omega\tau}, \tag{1}$$

where $\Delta\kappa'$ is the dispersion strength ($\Delta\kappa' = \kappa'_0 - \kappa'_\infty$), $\omega$ is the angular frequency, $\tau$ is the relaxation time and $i = \sqrt{-1}$. It is easily shown that using a definition of dielectric constant, $\kappa^* = \kappa' - i\kappa''$, eq. (1) is written into an equation of circle with its radius of $\Delta\kappa'/2$, and if we plot $\kappa''$ against $\kappa'$ in the complex plane, points obeying the Debye equation fall on a semi-circle as COLE and COLE (1941) first pointed out. The points where this plot touches the real axis correspond to the static and high-frequency limits of the dielectric constant.

Static dielectric constants of cores shallower than 55 m were determined from the Cole-Cole plots and those of cores deeper than 55 m from extrapolation of

frequency dependence curves as shown in Figs. 1, 3, and 4.

*3.4. Dielectric relaxation time*

Fig. 6 gives the frequency dependence of loss factor for the Mizuho cores with a reference curve of pure monocrystalline ice measured at −26.4°C and ordinary atmospheric pressure, $\sim 1 \times 10^5$ Pa. The cores taken from depths shallower than 55 m show clear maxima at a frequency around 10 kHz, which is a natural consequence of their dispersions having a single relaxation time as mentioned above, but it should be noted that their dispersion frequency is by an order of magnitude larger than that of pure monocrystalline ice. On the other hand, the cores taken from depths deeper than 55 m do not show a clear maximum in the plot of loss factor against frequency (Fig. 6).

Dielectric relaxation time ($\tau$) is defined as the reciprocal of dispersion frequency at which the loss factor has a maximum, and is usually determined graphically in such a plot as Fig. 6. In the present experiment, however, loss factors were not measured at so many points of frequency as to be able to find a maximum point; alternatively another method used by MAENO (1971, 1973a) to obtain relaxation times

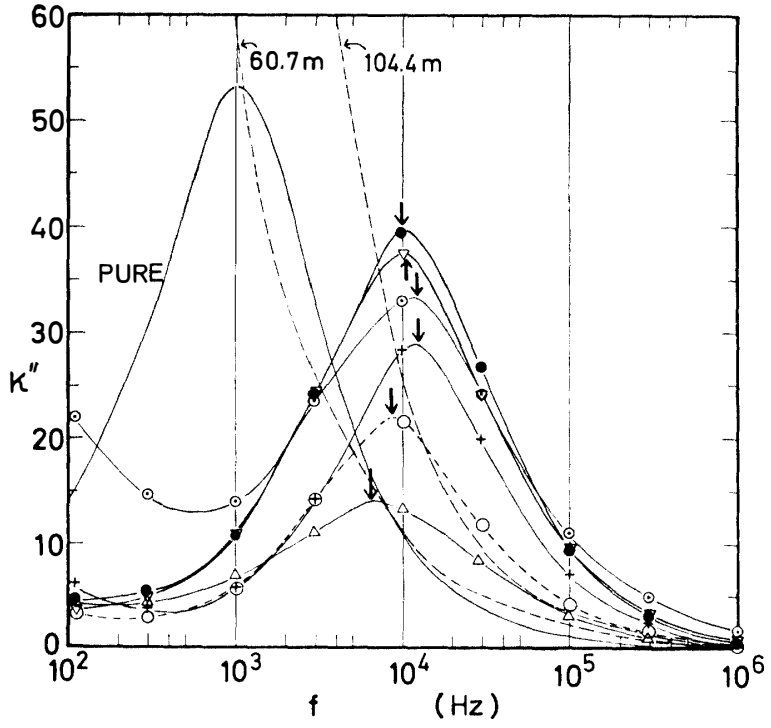


*Fig. 6. Frequency dependence of loss factor ($\kappa''$) for cores of different depths and pure monocrystalline ice (−26.4°C). Temperatures of measurements are the same as given in Figs. 1 and 5. Arrows indicate maximum points the frequencies of which were calculated from relaxation times obtained by using eq. (2). Depths are 7.8 m (△), 10.9 m (○), 19.6 m (+), 31.1 m (⊙), 40.3 m (●), and 50.3 m (▽).*

of KCl-doped ice was employed. The Debye equation, eq. (1), is written in the forms of

$$\kappa' - \kappa'_\infty = \frac{1}{\tau}\frac{\kappa''}{\omega} \tag{2}$$

and

$$\kappa'_0 - \kappa' = \tau(\kappa''\omega), \tag{3}$$

therefore, if we plot $\kappa''/\omega$ or $\kappa''\omega$ against $\kappa'$, relations of eqs. (2) and (3) are represented with straight lines and their slopes give the relaxation time. Fig. 7 is an example of such a plot of eq. (2) with data for a core of 19.6 m. The relations of eqs. (2) and (3) hold only in a narrow range of $\kappa'$ because of the increased effects of low-frequency polarizations.

The obtained relaxation times are given in Fig. 8 against the reciprocal of the absolute temperature. The straight line relationship means that the relaxation time can be represented as

$$\tau = \tau_0 \exp(E/kT) \tag{4}$$

where $\tau_0$ is a constant, $E$ is the activation energy and $k$ is the Boltzmann constant. $E$ was calculated from slopes of straight lines in Fig. 8 and the average values were $0.20\pm0.02$ eV ($19.3\pm1.5$ kJ·mol$^{-1}$) and $0.19\pm0.02$ eV ($18.4\pm1.5$ kJ·mol$^{-1}$) for cores shallower and deeper than 55 m, respectively. These values are much smaller than a value reported for pure ice, namely 0.574 eV (55.4 kJ·mol$^{-1}$, AUTY and COLE, 1952), suggesting the different mechanisms of dielectric polarization in the Antarctic core ice.

The dielectric dispersion, of which the relaxation time was calculated above, is the one appearing in the highest frequency range investigated in the present measurements. It should be noted that the high-frequency dispersion found in the

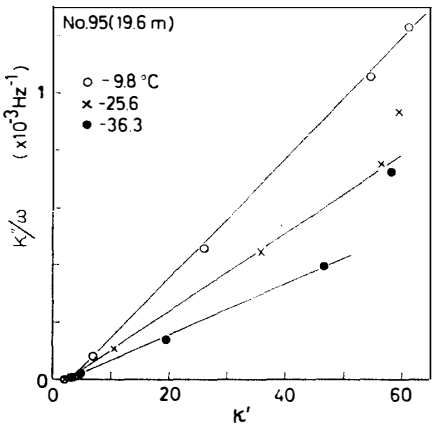


*Fig. 7. Plot of $\kappa''/\omega$ against $\kappa'$ for a core sample of 19.6 m.*

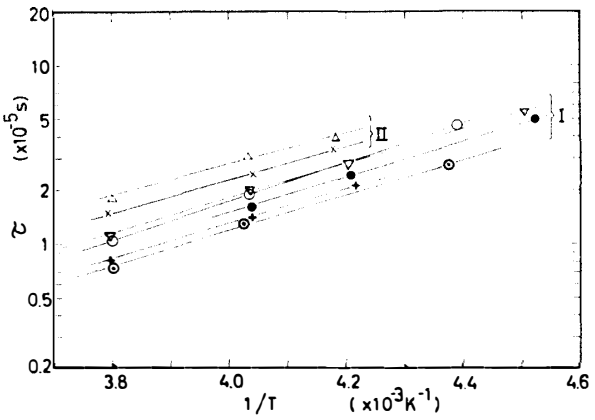


*Fig. 8. Temperature dependence of relaxation time ($\tau$) for cores of different depths: ○ (10.9 m), + (19.6 m), ⊙ (31.2 m), ● (40.3 m), ▽ (48.4 m), △ (120.9 m), × (124.3 m). I and II indicate cores taken from depth shallower and deeper than 55 m, respectively.*

cores deeper than 55 m is different from the one which gives the extremely large values of dielectric constant as mentioned in Section 3.3. The observed curves of dielectric dispersion for these deeper cores seem to be composed of at least two different dispersions, *i.e.*, the high-frequency dispersion and another more predominant one extending in lower frequencies.

### *3.5. High-frequency conductivity*

Limiting high-frequency conductivities were obtained graphically from frequency dependence curves as shown in Fig. 2, and plotted against the reciprocal of the absolute temperature in Fig. 9. The obtained values for cores shallower than 55 m are rather larger than those deeper than 55 m, as noted previously in Section 3.1. The larger conductivity seems to be associated with the petrographic structures of the cores, *i.e.*, small grain sizes and accordingly large inner free surface areas enabling the predominant surface conduction. This will be discussed in more detail in Section 4.3.

On the other hand, the smaller conductivities for cores deeper than 55 m are in agreement with those for deep cores drilled at Byrd Station (MAENO, 1974a), which are expressed with the empirical equation obtained by PAREN (1973) for deep cores from Camp Century and Site 2,

$$\sigma_\infty = \sigma_\infty^0 \exp\left(-\frac{E}{R}\left[\frac{1}{T}-\frac{1}{T_0}\right]\right) \tag{5}$$

where $T$ is the temperature, $R$ is the gas constant, and $\sigma_\infty^0 = 4.50\times10^{-5}\Omega^{-1}\mathrm{m}^{-1}$, $E=0.25$ eV (24.6 kJ·mol$^{-1}$) and $T_0=273.1$ K. The average activation energies for the high-frequency conduction were calculated from slopes of straight lines in Fig. 9 as $0.21\pm0.02$ eV ($20.3\pm1.5$ kJ·mol$^{-1}$) and $0.23\pm0.02$ eV ($22.2\pm1.5$ kJ·mol$^{-1}$) for cores shallower and deeper than 55 m, respectively. These values are slightly smaller

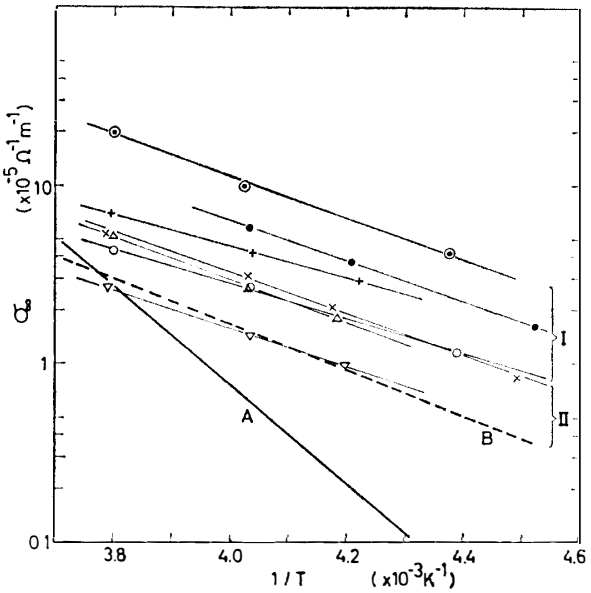


*Fig. 9. Temperature dependence of the high-frequency conductivity ($\sigma_\infty$) for the Mizuho cores at different depths:* ○ *(10.9 m),* + *(19.6 m),* ⊙ *(31.2 m),* ● *(40.3 m),* ▽ *(60.8 m),* △ *(120.9 m),* × *(124.3m). I and II indicate cores above and below 55 m respectively. The straight line* **A** *denotes $\sigma_\infty$ for pure ice with activation energy of 0.59 eV, and straight line* **B** *denotes the results of* PAREN *(1973) for deep cores from Camp Century and Site 2 in Greenland.*

than the Paren's value but almost the same as the activation energy obtained from the relaxation time in the previous section.

*3.6. Direct-current conductivity*

The d.c. conductivity of the Mizuho cores did not show clear dependence upon the depth, which is considered to be caused partly by the difficulties in fixing the specimen to the electrodes to get an ideal ohmic contact. Just as already mentioned in Section 3.1. about the small values of low-frequency conductivity (Fig. 2), the d.c. conductivities for cores shallower than 55 m were smaller than those for deeper cores; the values at $-10$°C were roughly $10^{-10}$—$10^{-7}\,\Omega^{-1}m^{-1}$ for the former and $10^{-8}$—$10^{-5}\,\Omega^{-1}m^{-1}$ for the latter, and the activation energy ranged form 0.40 eV (38.2 kJ·mol$^{-1}$) to 1.36 eV (131.5 kJ·mol$^{-1}$).

Such small d.c. conductivities for the shallower cores were also reported by KOPP (1962), who investigated five core samples, 10 to 50 m in depth, collected from the Greenland ice sheet and obtained fairly small conductivities compared with those of firn samples of the same density, *e.g.*, $7\times10^{-9}\,\Omega^{-1}m^{-1}$ at $-10$°C with the activation energy of 0.82 eV (79.2 kJ·mol$^{-1}$) for a core sample of 570 kg·m$^{-3}$. He also reported that the d.c. conductivity did not show any dependence upon density and depth.

## 4. Discussion

It has been shown in the previous sections that the Mizuho cores can conveniently be divided into two groups with respect to their dielectric properties, namely cores taken from depths shallower and deeper than 55 m. According to the measurements of air permeability of the Mizuho cores by MAENO *et al.* (1978) the former corresponds to permeable cores and the latter to impermeable cores, and it seems reasonable that the dielectric properties change at the critical density of 840 $kg \cdot m^{-3}$ (55 m), since at this density the intercommunicating air pores are completely closed off so that the densification mechanisms and microphysical conditions in the cores also alter.

### *4.1. Dielectric properties of permeable Mizuho cores*

Dielectric properties of permeable cores can be understood as those of a heterogeneous mixture dielectric composed mainly of two different components, *i.e.*, ice and air, and in principle the dielectric properties are determined by those of the components and their volume fractions. However, it is not easy to derive a formula as stated above because of difficulties arising from various complicated effects of size, shape, bonding or distribution of the composing materials on the formulation. Therefore, a number of different forms of empirical formulas have been proposed and used in different research fields (BEEK, 1967), but these many formulas can be expressed in general as

$$f(\kappa')=v_1 f(\kappa_1')+(1-v_1)f(\kappa_2') \tag{6}$$

where $\kappa'$, $\kappa_1'$, and $\kappa_2'$ are dielectric constants of the mixture dielectric, components 1 and 2, and $v_1$ is the volume fraction of the component 1. As for $f(\kappa')$, any of linear function, linear fractional function, power function and logarithmic function is frequently used, and it is theoretically proved that the maximum and minimum dielectric constants of mixture dielectric are given by eq. (6) when the form of the function is put as $f(\kappa')=\kappa'$ and $f(\kappa')=1/\kappa'$, respectively. Putting the static dielectric constants of ice and air as $\kappa_{0i}'$, and unity, respectively, and the volume fraction of ice and porosity as $v_i$ and $p$, respectively, we get the theoretical maximum of static dielectric constant ($\kappa_0'$) as

$$\kappa_0'=v_i\kappa_{0i}'+(1-v_i)=(1-p)\kappa_{0i}'+p. \tag{7}$$

Fig. 10 shows the plot of the observed static dielectric constants against the bulk density ($\rho$) and porosity ($p$) of the cores. The hatched band gives the region of theoretical maximum, which was calculated from eq. (7) by using values of $\kappa_{0i}'=95$ and 105 as two extremes for static dielectric constant of "ideal" Antarctic ice containing no macroscopic voids and bubbles. It is shown in this figure that the increase in $\kappa_0'$ with depth is definitely associated with the increase in the density, and that the observed values of $\kappa_0'$ gradually approach to those of theoretical maximum

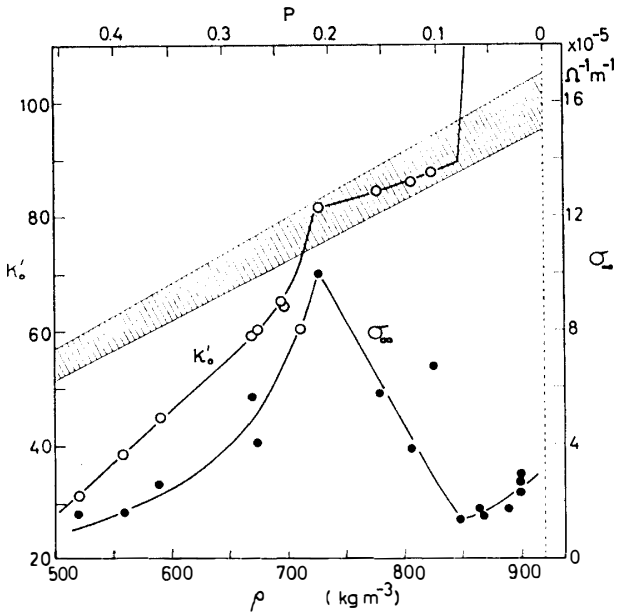


*Fig. 10. Plot of static dielectric constant ($\kappa_0'$) and high-frequency conductivity ($\sigma_\infty$) against the bulk density ($\rho$) and porosity ($p$). The hatched region gives the theoretical maximum of the static dielectric constant of the ice-air mixture according to eq. (7) when the static dielectric constant of ice ($\kappa_{0i}'$) is taken to range from 95 to 105.*

with increased density and reach them at a density of 730 kg·m$^{-3}$ which corresponds to 30 m in depth. The increase with density implies that the main mechanism of dielectric polarization of the permeable cores is afforded by the composing ice material itself, and the approach to the hatched band suggests that the internal texture of cores, including bonding and distribution of constituent ice particles, is changing to the state as indicated by eq. (7) with increasing density. This development of the internal texture reaches its maximum state at the critical density of 730 kg·m$^{-3}$, as was reported earlier (MAENO, 1974a, 1974b).

Above 730 kg·m$^{-3}$ the observed static dielectric constants lie within the maximum band (Fig. 10), showing that the mode of compaction of the cores is of the most ideal with respect to the dielectric properties. This finding that the bonding structure of cores develops with the increase of density and reaches some optimum state at 730 kg·m$^{-3}$ gives valuable information about the structural process and mechanism of densification of polar firn, as will be discussed with reference to other petrofabric analyses in Section 4.3.

The most dominant dielectric dispersion found in permeable Mizuho cores is represented fairly accurately by the Debye equation with a single relaxation time as manifested in Fig. 5. Since the static dielectric constant of the Debye type dispersion increased with increasing density and approached the theoretical maximum expected from the model of mixture dielectric composed of air and ice, the Debye

dispersion is considered as due to the bulk relaxation of the composing ice, in which the polarizations are caused by the reorientations of water molecules through the movements of Bjerrum defects.

On the other hand, the relaxation time of the permeable core is shorter by an order of magnitude than that of laboratory grown pure ice, and the activation energy ($0.20\pm0.02$ eV) for the relaxation time and that for high-frequency conduction ($0.21\pm0.02$ eV) are only half of those for the pure ice. This suggests that other mechanisms are also contributing in addition to those taking place within the composing ice.

A possible explanation is the presence of ice-air interfaces in the cores as suggested by PAREN and GLEN (1978) since water molecules near such an interface are considered to be more mobile to reorient and be able to give rise to dielectric response (MAENO and NISHIMURA, 1978). Similar results were also found in the solid mixture of ice and KCl particles at temperatures below the eutectic point ($-11°C$) of $H_2O$-KCl system (MAENO, 1973a, p. 21); the relaxation time of dielectric dispersion was much shorter than that of pure ice and its activation energy was 0.230 eV (22.3 $kJ\cdot mol^{-1}$). The results were tentatively attributed to the presence of impurities though detailed mechanisms were not certain.

Now it seems probable that the Debye dispersion appearing dominantly at high frequencies in the permeable cores and also in the solid ice-KCl mixtures should be produced by combination of the orientational polarizations of water molecules in the composing ice itself and the so-called Maxwell-Wagner effects occurring at numerous internal surfaces and grain boundaries which provide ample electric discontinuities to give rise to electric polarizations; impurities are considered in general to reinforce the polarizations by introducing more mobile change carriers in the ice and near the free surfaces and grain boundaries of ice particles. The analyses to examine the concept and to distinguish the polarizations taking place within the ice itself and at internal free surfaces and grain boundaries, are urgently required.

It should be worthwhile to mention here that besides the dominant dispersion discussed above and that appearing at frequencies lower than about 50 Hz, no other dielectric dispersions could be detected for the permeable Mizuho cores in the frequency range investigated in the present study. This suggests that even though there had ever existed other dispersions they have disappeared in the tremendously long annealing period within the Antarctic ice sheet.

In Fig. 10 the limiting high-frequency conductivity ($\sigma_\infty$) is also plotted; the conductivity increases with increasing density until $730\,kg\cdot m^{-3}$, and at higher densities the conductivity decreases to about $3\times10^{-5}\Omega^{-1}m^{-1}$. The variation of $\sigma_\infty$ seems to be explained by the formation and diminishment of small air voids during the densification process, as will be mentioned in Section 4.3.

*4.2. Dielectric properties of impermeable Mizuho cores*

Dielectric properties of the impermeable Mizuho cores, namely cores recovered from depths deeper than 55 m and with densities higher than 840 $kg \cdot m^{-3}$, are characterized by large values of dielectric constant and conductivity and by wide frequency range of dielectric dispersion compared with those of laboratory pure ice. These behaviors are essentially similar to those of impermeable deep cores from Byrd Station (MAENO, 1974a, 1974b; FITZGERALD and PAREN, 1975) and from Amery Ice Shelf (MAENO, 1974a, 1974b), and it is likely that the same electrical mechanisms are responsible for the unusual properties observed in these polar glacier ices.

Static dielectric constants are by orders of magnitude larger than the theoretical maximum expected from eq. (7) as given in Figs. 1, 4, and 10, so that the dielectric properties of the impermeable cores cannot be accounted for with a simple theory of mixture dielectrics, but to be explained by different mechanisms. Examining the probable mechanisms such as electrode polarizations, impurities contained, hydrostatic pressures and formation of clathrate hydrates of air, MAENO (1974a, 1974b) concluded that the unusual dielectric behaviors of deep polar ice might be caused by mechanical strains stored locally in the core samples; strains may produce various kinds of structural imperfections such as point defects, dislocations and stacking faults, which would increase the number of charge carriers, possibly $H_3O^+$ ions.

The effects of impurities contained were not regarded to be the main cause of the unusual electrical behaviors, since the impurity level was extremely low: the electrical conductivity of the melt of the deep core samples was as low as $(3\text{–}6) \times 10^{-4}$ $\Omega^{-1}m^{-1}$ at $+25°C$, which was comparable to that of distilled water in laboratories. However, according to the neutron activation analyses by MUROZUMI and PATTERSON (1970), Arctic and Antarctic deep cores contain chlorine impurities amounting to $(0.9\text{–}2.0) \times 10^{-6}$ $mol \cdot kg^{-1}$. This impurity level is not low enough to be disregarded in considering the electrical and other structure-sensitive properties of deep polar ice.

It has been reported that chlorine impurities can be incorporated substitutionally into the crystal lattice of ice to an extent of $1 \times 10^{-4}$ $mol \cdot kg^{-1}$ to result in the alteration of dielectric properties of the chlorine doped monocrystalline ice (MAENO, 1973a, 1973b); small amounts of chlorine impurities, trapped at grain boundaries possibly together with other cations such as potassium and sodium, increase the dielectric constant and conductivity enormously at temperatures below the eutectic point. This effect was observed to be most effective at concentrations of $10^{-4}$ to $10^{-3}$ $mol \cdot kg^{-1}$ with the activation energy of high-frequency conductivity of 0.230 eV (22.3 $kJ \cdot mol^{-1}$) comparable to that for the impermeable polar ice (MAENO, 1973a, p. 26).

Furthermore, it is expected that the substitutional or interstitial incorporation of chlorine and other impurities in the ice lattice may be reinforced in the abnormal

condition of long ageing period under high pressure, high homologous temperature and complex mechanical strain in the polar ice sheet, and may generate more effectively the electrical active imperfections such as D, L, $H_3O^+$, $OH^-$ and possibly other unknown defects.

By mechanical strains we mean every sort of stress disturbances within the deep polar ice; the densification or compaction of polar ice above the critical density of 840 $kg \cdot m^{-3}$ is believed to proceed through shrinkage of closed-off air bubbles, resulting in the increase in pressure inside and dissolution of molecules of air into the surrounding ice lattices. This process is of course extremely slow but the internal stress and flow systems are certainly complicated as suggested for example by the petrofabric results of the deep Mizuho cores (NARITA *et al.*, 1978), in which the fabric patterns, size and shapes of crystal grains vary irregularly as the depth changes.

We should also pay attention to a possibility of generation of mechanical strains in the cores when they were recovered from the high pressure depths to the surface of normal pressure. The stress relaxation in the storing time after the recovery has been reported by GOW (1971) for the Byrd deep cores, and the author observed that an impermeable Mizuho core taken out from 125 m in depth, containing many cracks, showed dielectric properties rather similar to those of laboratory pure ice, which seems to be accounted for by the relaxation due to the formation of cracks. However, we cannot distinguish between the dielectric properties due to mechanical strains artificially introduced on the recovery and those attributable to the intrinsic nature of polar ice. Therefore, more studies of the same kind as the present work on other polar regions are required together with the observations of polar ice sheets as they are.

*4.3. Bonding and densification characteristics of the Mizuho cores*

It has been reported frequently (PERUTZ and SELIGMAN, 1939; BENSON, 1962; ANDERSON and BENSON, 1963; LANGWAY, 1967) that snow deposits in cold polar regions undergo a densification process firstly of mechanical packing of voids with snow particles till a critical density of 550 $kg \cdot m^{-3}$, secondly of compaction by plastic deformation and recrystallization of composing ice crystals till 840 $kg \cdot m^{-3}$, and finally of the decrease of separate bubble volumes until the density of solid ice. On the other hand, our dielectric inspection of the Mizuho cores has revealed at the density of 730 $kg \cdot m^{-3}$ (about 30 m in depth) the presence of another clear transition, which suggests a completion and alteration of some densification process, which is discussed in some detail below.

In Fig. 11 static dielectric constants $\kappa_0'$ and high-frequency conductivity $\sigma_\infty$ are plotted against depth, together with the bulk density $\rho$, which was compiled by NARITA and MAENO (1978), and the specific areas of internal free surfaces (air-ice interfaces) $S_f$ and crystallogr aphic grain-boundaries $S_g$ in the unit of $m^2 \cdot m^{-3}$, which

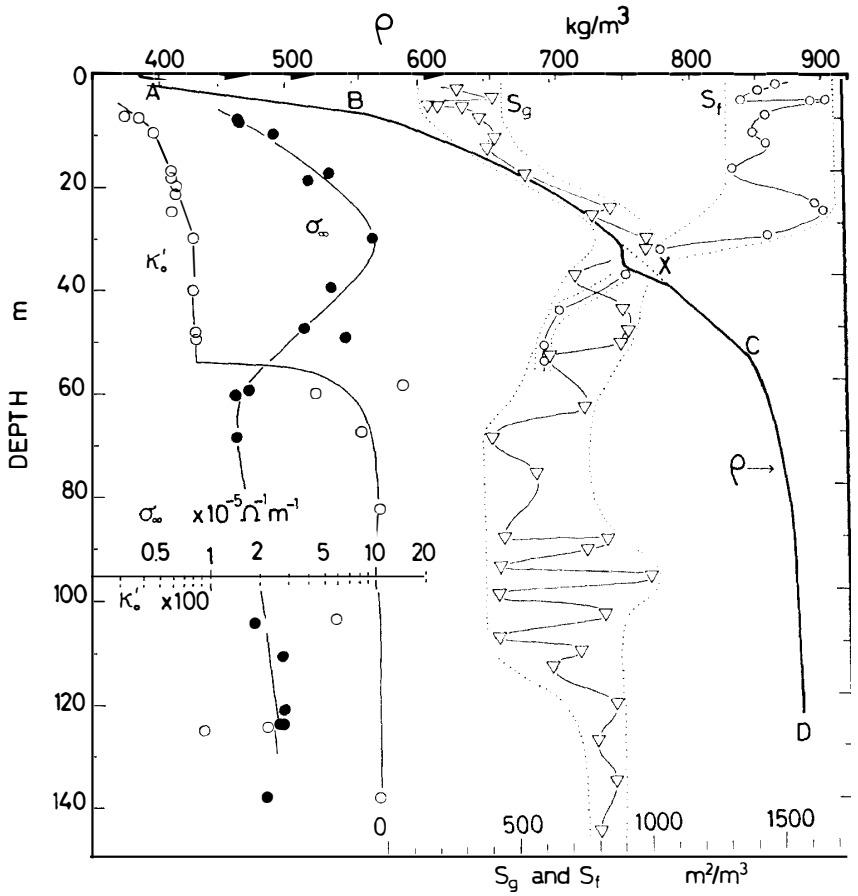


*Fig. 11. Variations with depth of static dielectric constant ($\kappa_0'$) and high-frequency conductivity ($\sigma_\infty$), with some other physical properties such as density ($\rho$) and specific areas of internal free surfaces ($S_f$) and crystallographic grain-boundaries ($S_g$).*

were calculated from photomicrographs of thin sections of cores, details of which are given in NARITA *et al.* (1978). $S_g$ increases with depth and reaches a maximum value of about 1000 $m^2 \cdot m^{-3}$ at the depth of 30 m. This depth dependence of $S_g$ is similar to that of $\kappa_0'$ and confirms the above explanation of optimum state of ice bonding, because the increase in $S_g$ corresponds to the development of bonding between constituent ice particles.

On the other hand, with increasing depth $S_f$ does not increase steadily, but fluctuates in a small range. This means that contained air voids split into numerous smaller ones to result in the formation of new internal free surfaces. These surfaces are considered to be the main cause of the increase in $\sigma_\infty$. At the depth of about 30 m, $S_f$ rapidly decreases. This may cause the rapid decrease in $\sigma_\infty$.

According to the analyses by MAENO *et al.* (1978) on the air permeability of snow at Mizuho and Site 2 in Greenland, the configuration of interconnecting air channels reaches some optimum state at porosity of 0.2, *i.e.*, at a density of 730 $kg \cdot m^{-3}$.

The petrographic analyses by NARITA *et al.* (1978) have also revealed that the various structural characteristics change at the critical density. These results, in conjunction with those of the present work, suggest that the optimum texture of snow at the critical density is such that contacts between adjacent ice particles are maximum and air channels are concentrated only at intersections of grain boundaries.

The density profile also shown an abnormal deviation from a smoothed line at the depth 30–40 m (Fig. 11), which may be associated with the above-mentioned petrographic development of snow structures. Though there is not enough information available for determining what is the most important factor to generate such most ideal bonding of ice particles in a density range between 550 and 840 $kg \cdot m^{-3}$, the density region around 730 $kg \cdot m^{-3}$ seems to have some unique significance in the densification mechanism. The concept is expected to be examined in other ice sheets.

## Acknowledgments

The author is indebted to Prof. A. HIGASHI and Dr. Y. SUZUKI of Hokkaido University and Prof. K. KUSUNOKI of the National Institute of Polar Research for comments given to the present paper. The author is also indebted to Mrs. Y. UEMATSU, Mr. H. NARITA, Mr. K. ARAOKA, and Mr. Y. KANEDA for their assistance in preparing the manuscript.

The expence of this study was partly defrayed from a Special Fund for Scientific Research of the Ministry of Education, Science and Culture, Japan.

## References

ANDERSON, D. L. and BENSON, C. S. (1963): The densification and diagenesis of snow. Ice and Snow, Properties, Processes and Applications, ed. by W. D. KINGERY. Cambridge, The M.I.T. Press, 391–409.

AUTY, R. P. and COLE, R. H. (1952): Dielectric properties of ice and solid $D_2O$. J. Chem. Phys., **20**, 1309–1314.

BEEK, L. K. H. VAN (1967): Dielectric behaviour of heterogeneous systems. Progress in Dielectrics, ed. by J. B. BIRKS *et al.* London, Heywood Books, **7**, 71–114.

BENSON, C. S. (1962): Stratigraphic studies in the snow and firn of the Greenland ice sheet. SIPRE Res. Rep., **70**, 139 p.

COLE, K. S. and COLE, R. H. (1952): Dispersion and absorption in dielectrics. I. Alternating characteristics. J. Chem. Phys., **9**, 341.

FITZGERALD, W. J. and PAREN, J. G. (1975): The dielectric properties of Antarctic ice. J. Glaciol., **15**, 39–48.

GOW, A. J. (1971): Relaxation of ice in deep drill cores from Antarctica. J. Geophys. Res., **76**, 2533–2541.

KOPP, M. (1962): Conductivité électrique de la neige, au courant continu. J. Math. Phys. Appl., **13**, 431–441.

LANGWAY, C. C., Jr. (1958): Bubble pressure in Greenland glacier ice. Int. Assoc. Hydrol., Pub. **47**, 336–349.

LANGWAY, C. C., Jr. (1967): Stratigraphic analysis of a deep ice core from Greenland. CRREL Res. Rep., **77**, 127 p.

MAENO, N. (1971): Enka-kariumu gôri no yûden bunsan III. (The dielectric dispersion of KCl ice. III. The dielectric dispersion of high-concentration ice). Teion Kagaku, Butsuri-Hen (Low Tem. Sci., Ser. A, Phys.), **29**, 1–10.

MAENO, N. (1972): Dielectric properties of KCl ice. J. Appl. Phys., **43**, 312–316.

MAENO, N. (1973a): Studies of the dielectric properties of ice grown from KCl solution. Contrib. Inst. Low Temp. Sci., Hokkaido Univ., Ser. A, **25**, 47 p.

MAENO, N. (1973b): Single crystals of ice grown from KCl solution and their dielectric properties. Can. J. Phys., **51**, 1045–1052.

MAENO, N. (1974a): Investigations of electrical properties of deep ice cores obtained by drilling in Antarctica. Kyokuchi Hyôshô-gôri no Butsuri-teki Kagaku-teki Kenkyû (Physical and Chemical Studies on Ices from Glaciers and Ice Sheets), ed. by D. KUROIWA. Sapporo, Inst. Low Temp. Sci., Hokkaido Univ., 45–56.

MAENO, N. (1974b): Kyokuchi no kôri no denki-teki seishitsu I (Electrical properties of polar ice. I). Teion Kagaku, Butsuri-Hen (Low Temp. Sci., Ser. A, Phys.), **32**, 25–38.

MAENO, N. and NISHIMURA, H. (1978): The electrical properties of ice surfaces. To be published in J. Glaciol., **21** (85).

MAENO, N., NARITA, H., and ARAOKA, K. (1978): Measurements of air permeability and elastic modulus of snow and firn drilled at Mizuho Station, East Antarctica. Mem. Natl Inst. Polar Res., Spec. Issue, **10**, 62–76.

MUROZUMI, M. and PATTERSON, C. C. (1970): Nanboku ryôkyoku hyôsetsu-chû no enso no hôsha-ka bunseki (Neutron activation analysis of chlorine in Antarctic and Arctic snow and ice). Bunseki Kagaku (Analytical Chemistry), **19**, 1049–1056.

NARITA, H. and MAENO, N. (1978): Compiled density data from cores drilled at Mizuho Station. Mem. Natl Inst. Polar Res., Spec. Issue, **10**, 136–158.

NARITA, H., MAENO, N. and NAKAWO, M. (1978): Structural characteristics of firn and ice cores drilled at Mizuho Station, East Antarctica. Mem. Natl Inst. Polar Res., Spec. Issue, **10**, 48–61.

PAREN, J. G. (1973): The electrical behavior of polar glaciers. Physics and Chemistry of Ice, ed. by E. WHALLEY *et al.* Ottawa, Royal Society of Canada, 262–267.

PAREN, J. G. and GLEN, J. W. (1978): Electrical behaviour of finely divided ice. To be published in J. Glaciol., **21** (85).

PERUTZ, M. and SELIGMAN, G. (1939): A crystallographic investigation of glacier structure and mechanism of glacier flow. Proc. R. Soc. London, Ser. A, **172**, 335–359.

RÖTHLISBERGER, H. (1967): Electrical resistivity measurements and soundings of glaciers: introductory remarks. J. Glaciol., **6**, 599–606.

*(Received May 25, 1978; Revised manuscript received September 4, 1978)*